First Generation Acrylic Encapsulated U/Th Sources

Steve Brice[1], Xi Chen[3], Fraser Duncan[4], Malcolm Fowler[2], Andrew Hime[1], Geoff Miller[2], Jerry Wilhelmy[2]
1. P-23 LANL 2. CST-11 LANL
3. LBNL 4. Queens University

SNO-STR-99-023

February 21, 2000

Contents

1 Introduction

This document gives details of the first generation acrylic encapsulated U/Th sources that have been constructed to give information on the decays of ^{208}Tl and ^{214}Bi in the detector. The activities within these sources are ^{232}U which decays with 68.9 year halflife to join the Th chain at ^{228}Th, and ^{226}Ra which is part of the U chain and has a 1599 year halflife. In their existing form these sources were only ever designed to be prototypes. The intention was always that the information gathered by placing these sources in the detector would be used to construct better, second generation sources. In fact since the construction of the sources the goalposts have been moved and we now have tasks for these sources that we know *a priori* the first generation will not be able to fulfill. This will be made clear in the sections that follow. Currently there are three goals for acrylic encapsulated sources

- Produce data sets that look as much like free ^{208}Tl and ^{214}Bi decays in water as possible in order to have isotropy PDFs that Xin Chen's background analysis technique can use. (More on this in later sections).
- Produce data sets that look as much like free ^{208}Tl and ^{214}Bi decays in water in order to see just what the Cerenkov background wall looks like.
- Test the performance of fitters on ^{208}Tl and ^{214}Bi decays.
- Verify the deuteron photodisintegration cross section at the γ energies we worry about.

It is unclear whether the first generation sources will meet any of these goals at the level we would like, but placing them in the detector should provide information enabling us to design next generation sources that do.

2 Hardware

2.1 Source Fabrication

Fabrication of the sources was done in several steps. The activity ($\leq$0.1 mL) was first placed in the bottom of the small inner cup. This cup is shown in Fig.1. Next, the solution was evaporated at about 80 °C for a few hours. The cup was then filled about half full with PS-30, which had been prepared with about half the normal amount of activator in order to extend its pot life. The PS-30 was also degassed before use. The PS-30 was allowed to set up overnight in a low temperature oven at about 35 °C . The small cup was then cleaned in an ultrasonic bath using alcohol, Alconox, and, finally, deionised water. This step was done to remove any possible activity that was not completely encapsulated

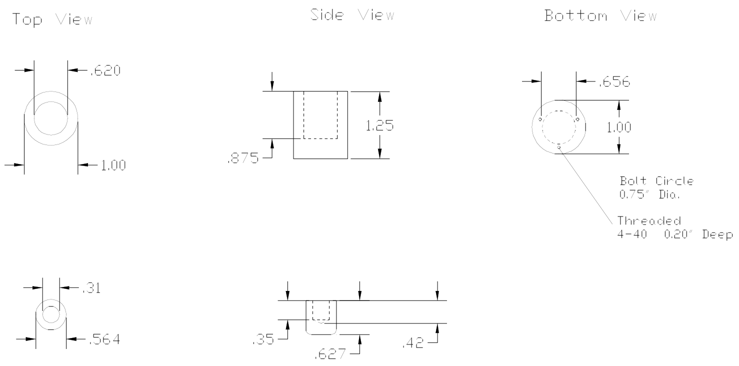

Material for both parts: UVT Acrylic
Dimensions are in inches
M. Fowler 7/19/99

Figure 1: The acrylic components from which the sources are constructed

within the PS-30. Next the small cup was filled with a (degassed) 50% slush of methyl methacrylate and PMMA powder. The slush was then allowed to cure overnight at 70 °C in an autoclave pressurised to 150 psia with nitrogen. The next day the temperature was raised to 95 °C for two additional hours. The cup was removed from the autoclave, cleaned again with the ultrasonic cleaner, and any excess polymer was removed from the top of the cup. Next the outer container (shown in the upper part of Fig.1) was prepared by adding enough of the slush mixture to fill a depth of about 3mm. The small inner cup with the activity was then added, top down. After it was ensured that there were no bubbles between the inner and outer parts, enough additional slush was added to completely cover the inner part, but not fill the outer part completely. This was then cured in the pressurised autoclave in the same manner as before. After cleaning one more time, the source was overfilled with slush and again cured as before. Finally the source was machined to get smooth polished surfaces and then annealed at 100 °C in the pressurised autoclave for at least 4 hours.

Source	Height (cm)	Activity (June 1 1999)
^{226}Ra	2.99	63 2.45 MeV γs/sec
Hot ^{232}U	2.85	5350 2.6 MeV γs/sec
Weak ^{232}U	2.86	99 2.6 MeV γs/sec

Table 1: The measured source activities

2.2 Source Assay

After preparation the sources were γ counted to establish the decay rate. Counting was done on two different occasions and in several different counting geometries. It is hard to get a good estimate of the uncertainty in the activity since the counting statistics are considerably better than the systematics. The uncertainty estimates are about 10% for the strong sources and probably 15-20% for the weaker ones. The best estimates of the source activities are shown in Table 1. As an aside, if one assumes that the human hand weighs 250g and that a 2.6 γ will, on average, deposit 0.5 Mev when passing through a human hand. Then the dose received by someone holding the hottest of the three sources clasped in their hand for an entire year would be 5.4 mSv. This should be compared with the average annual dose in the U.S. from background radiation of 3.6 mSv.

2.3 Source Mounting

The source mounted on the manipulator is shown in Fig.2. The mounting scheme uses the laserball mounting hardware but replaces the laserball diffusing flask with an acrylic stem that has the source attached to the bottom. The support stem is shown in Fig.3. The source is attached to the acrylic stem via three 4-40 screws.

The advantage of using the laserball hardware is that it minimizes the time necessary to change between the laserball and acrylic encapsulated source. Using the laserball hardware also provides a means of securing the umbilical. Although the umbilical is not required for the operation of the acrylic source, it is a backup support mechanism in case of failure of the main support rope.

A possible failure mode that would result in the loss of the source in the detector is if the acrylic mounting stem for the source broke. To prevent loss of the source in this situation, a fine stainless steel wire "basket" will be woven around the source and then secured to the mounting hardware above the stem. In the event of failure of the stem, the source will remain attached to the manipulator and can be retrieved from the detector.

2.4 Handling Instructions

During and after fabrication the sources were cleaned in the manner described in Sec.2.1. It is also necessary, however, to clean the source before each insertion into the D_2O to remove any dust build up. The up to date version of these cleaning procedures can be found at

www.sno.phy.queensu.ca/private/calibration/procedures/cleaning.html

The procedures at the time of writing are reproduced below.

The basic philosophy is that you should clean the source before bringing it to site. If cleaned off site, bag it multiple times before travel. Once it is brought

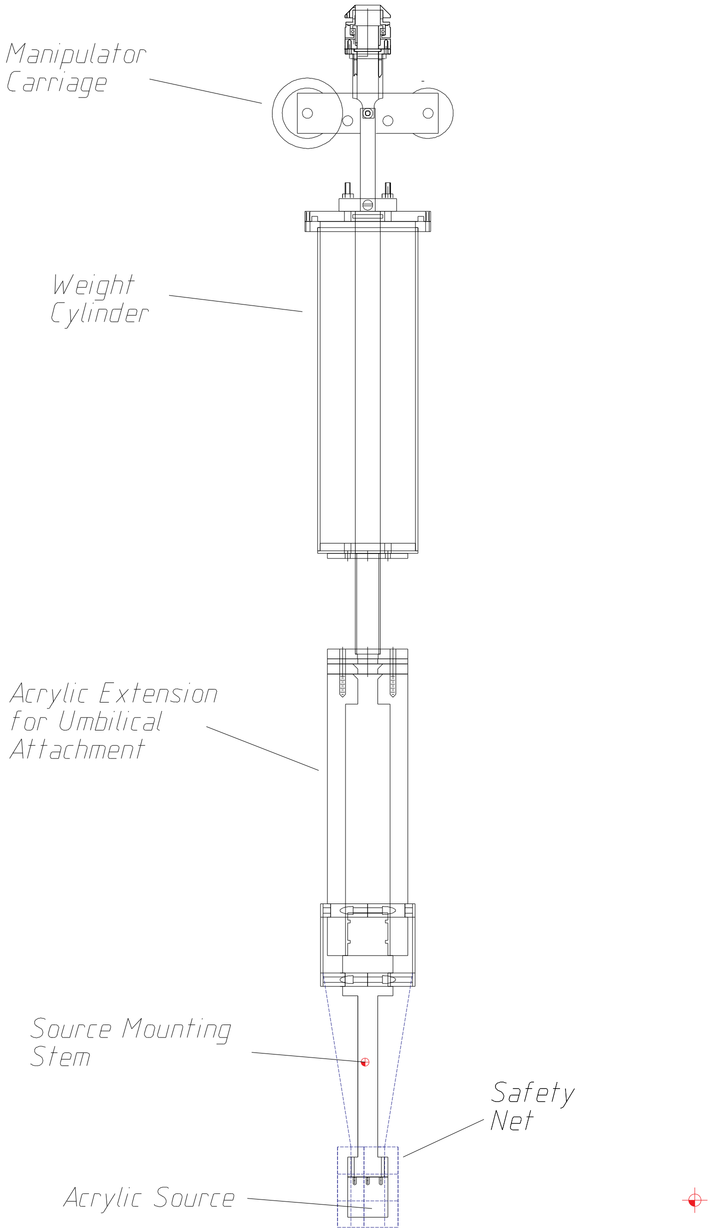

Figure 2: An acrylic source mounted on the manipulator

underground, it should probably be cleaned again. The hard rules for putting a source into the detector are:

1. Any material that comes in contact with the D_2O must be emanation tested and leach tested.

2. Any object going into the D_2O must be tape lifted and counted for mine

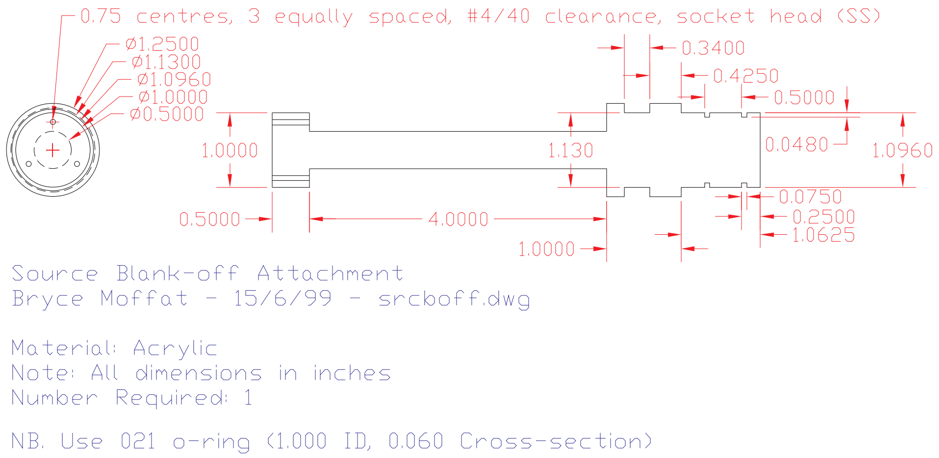

Figure 3: Detail of the source mounting stem

dust prior to going in. The counted dust levels must be below the levels specified by Hugh Evans.

3. If a source has been tape lifted, but its history since the tape lift is uncertain (not sure if it was stored properly etc.) another tape lift should be done.

There is a restriction on which chemicals are allowed on the deck - in particular solvents are a concern since they may attack the deck seals and make their way into either the light or heavy water. At present the only approved cleaning agents in the DCR are Alconox and ultrapure water. Outside the deck area, agents such as methanol can be used (in a manner consistent with usual safety practices).

In general the cleaning procedure is simple. The main rule to be aware of is that if you use a cleaning agent that leaves a residue (such as Alconox) it is necessary to clean the residue off with ultrapure water. Cleaning procedures that have been used on components are:

- Ultrasonic Cleaner: This is the best method for components such as stainless steel housings and complex metal parts that are hard to access (e.g. the manipulator carriages, weight assemblies, nuts, bolts).

  1. Several hours in hot water (40-60 °C) with detergent (don't know which types are good).
  2. One or more hours in hot ultrapure water to remove detergent residue.

- Alconox and Ultrapure Water: Objects like umbilicals are too soft for the ultrasonic cleaner to work. Also there are objects that are too delicate to put in an ultrasonic cleaner. For these objects
  1. Several wipes of the object with Alconox. Repeat until no detectable dirt is removed.
  2. Several wipes of the object with ultrapure water to remove the Alconox residue.

One note to add here is that the dust level limits refered to above are that all surfaces should have less than 0.5 micrograms/cm**2 of mine dust. This assumes that mine dust has approximately 5ppm Th and 3ppm U.

3 Source Simulations

In this section SNOMAN 3_0186 with its default optical constants is used to study the acrylic encapsulated sources. In all simulations the source is positioned at the center of the detector and the material used is SNOMAN's standard acrylic. The assumed geometry of the source is shown in Fig. 4. Events are set off from the small disk region indicated in the middle of the acrylic.

3.1 NHIT Spectra

Fig.5 shows the NHIT spectra for ^{214}Bi and ^{208}Tl from the source and from pure water. A fiducial volume cut of rfit $<$ 200cm is imposed. It is clear from these plots that both isotopes have their NHIT spectra shifted up by the presence of the acrylic, the ^{214}Bi more so than the ^{208}Tl. This is an effect of the higher refractive index of acrylic. The Cerenkov production rate by an electron per unit track length per unit wavelength is given by

$$\frac{\mathrm{d}^2\mathrm{N}}{\mathrm{dxd}\lambda} = \frac{2\pi\alpha}{\lambda^2}\left(1 \; - \; \frac{1}{n^2\beta^2}\right)$$

The refractive index difference between water (1.33) and acrylic (1.49) means that for a fully relativistic particle ($\beta = 1$) the acrylic will produce 26% more light per unit track length. This effect is reduced by the fact that the betas are not fully relativistic (the largest electron endpoint is 2.4 MeV) and by the fact that some of the light has its origin in γs which convert outside of the acrylic. This latter effect is the reason why, at the high NHIT end, the single electron from ^{214}Bi has its spectrum shifted up more than the electron and γ from ^{208}Tl. Another strong effect is the attenuation length of acrylic which is short enough to counteract somewhat the higher Cerenkov production of acrylic. This effect is illustrated by the NHIT spectra of Fig.6 where a larger source (radius 4cm,

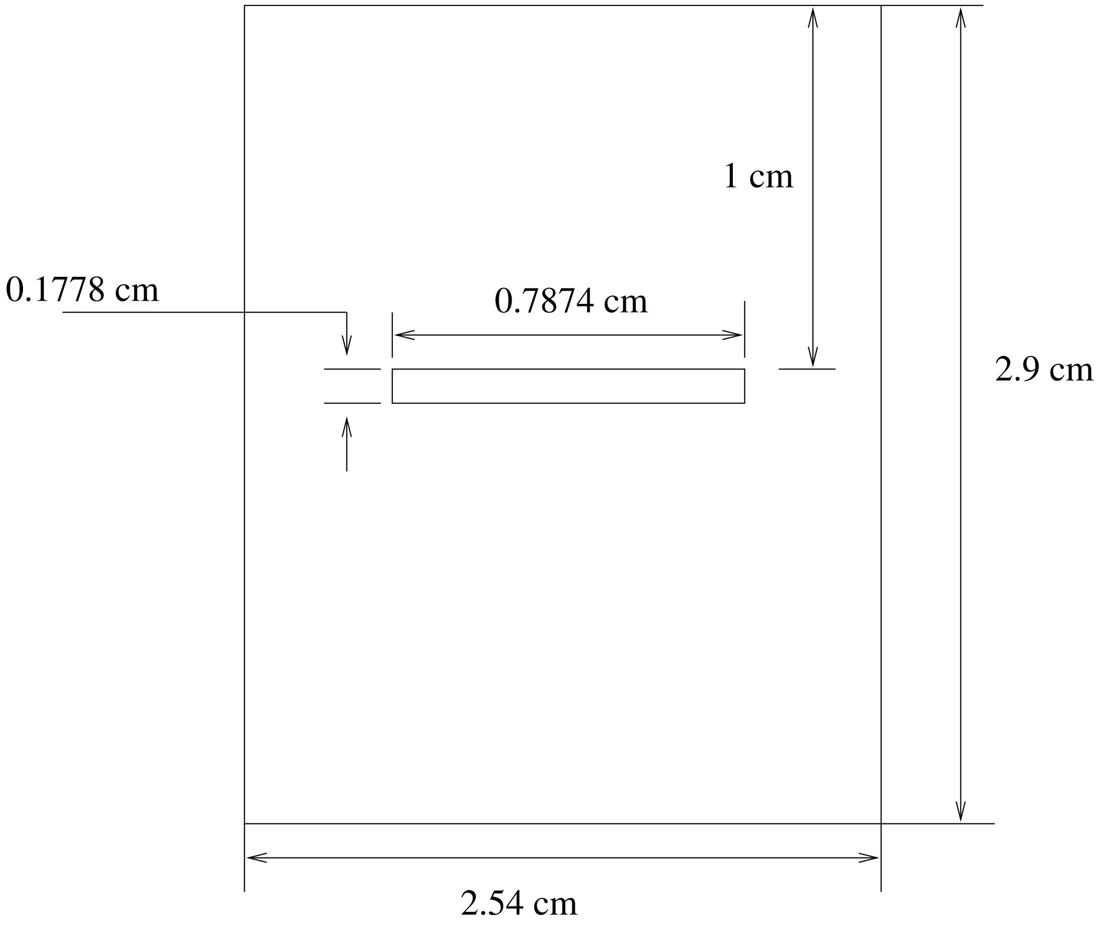

Figure 4: The source source geometry assumed in simulation

height 8cm) has been simulated. It exhibits upward shifts of the NHIT spectra, but the greater attenuation with a longer path through acrylic means that they are smaller than those of Fig.5.

It should be noted that, with the mean pathlength of a 5 MeV electron being 2cm in water, few if any of the electrons emitted by the acrylic encapsulated sources will make it out of the acrylic and into the water.

3.2 Isotropy

One of the primary uses of the low energy acrylic encapsulated sources will be to calibrate Xi Chen's techniques for distinguishing between ^{208}Tl and ^{214}Bi decays. The history of this technique traces back to Dave Wark's suggestion that the single electron from a CC interaction should produce a different PMT hit pattern than the multiple electrons that result from an NC interaction followed by capture on ^{35}Cl. This idea was pursued by Steve Brice who showed that the NC hit patterns were indeed more isotropic and this fact could be used to determine the number

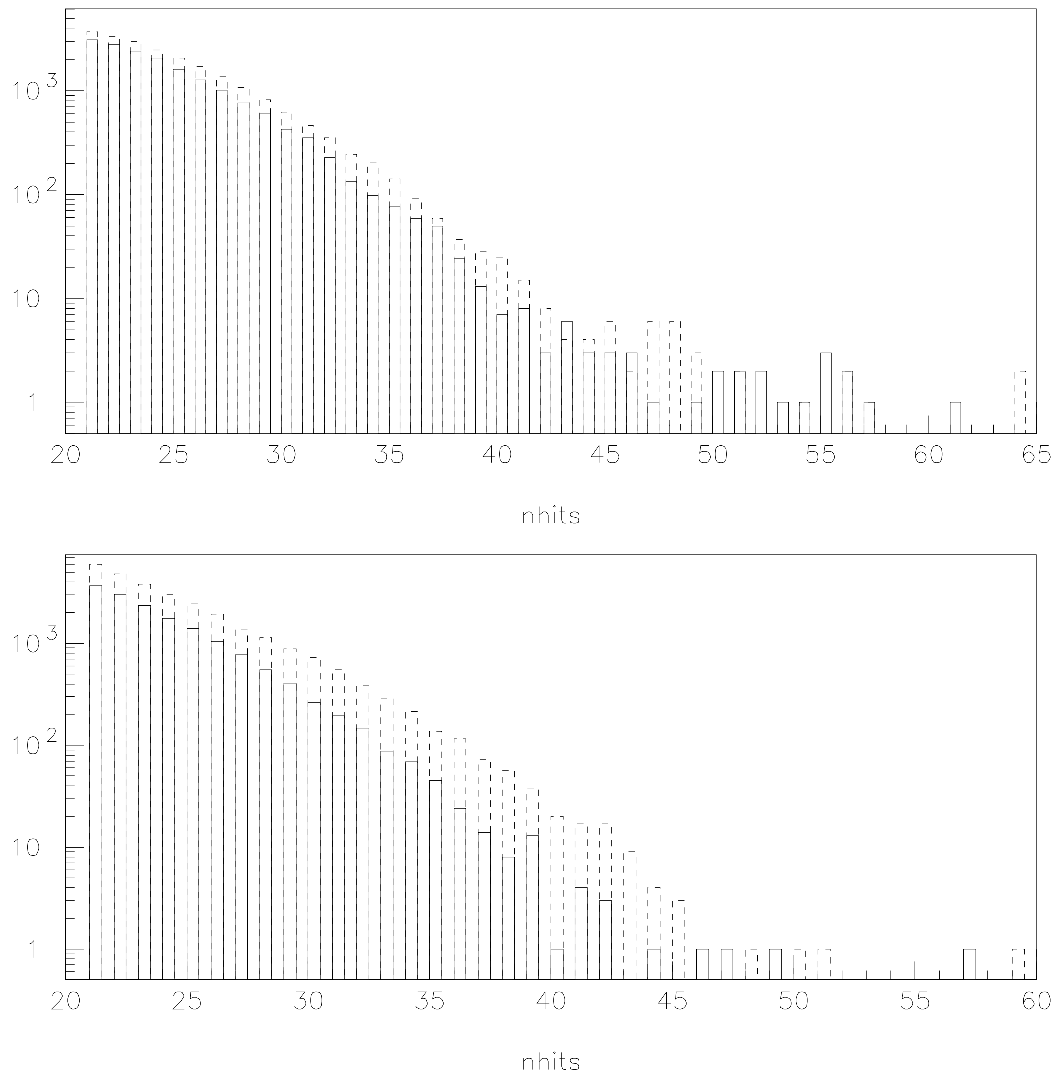

Figure 5: NHIT distributions for ^{208}Tl (upper plot) and ^{214}Bi (lower plot) decays with (dashed line) and without (solid line) acrylic source.

of CC and NC interactions in a data set on a statistical basis (as opposed to the event by event level). Martin Moorhead then noticed that a similar distinction between single and multiple electrons exists near the endpoints of ^{208}Tl and ^{214}Bi. To reach reasonably high NHIT a ^{214}Bi has to proceed through a single β to the daughter ground state, with no γs (γs are less efficient at producing hits than βs of the same energy). The β must, in addition, be in the upper part of its energy spectrum. ^{208}Tl on the other hand can reach high NHITs with a moderate energy β, possibly some low energy γs and the 2.6 MeV γ that is always present: in other words multiple electrons. Xin Chen took this idea and showed that

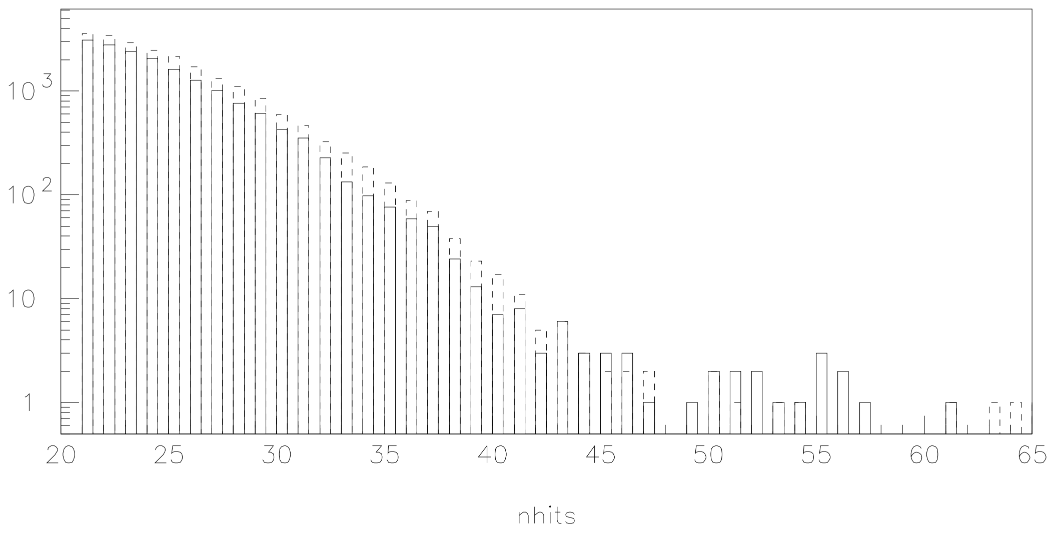

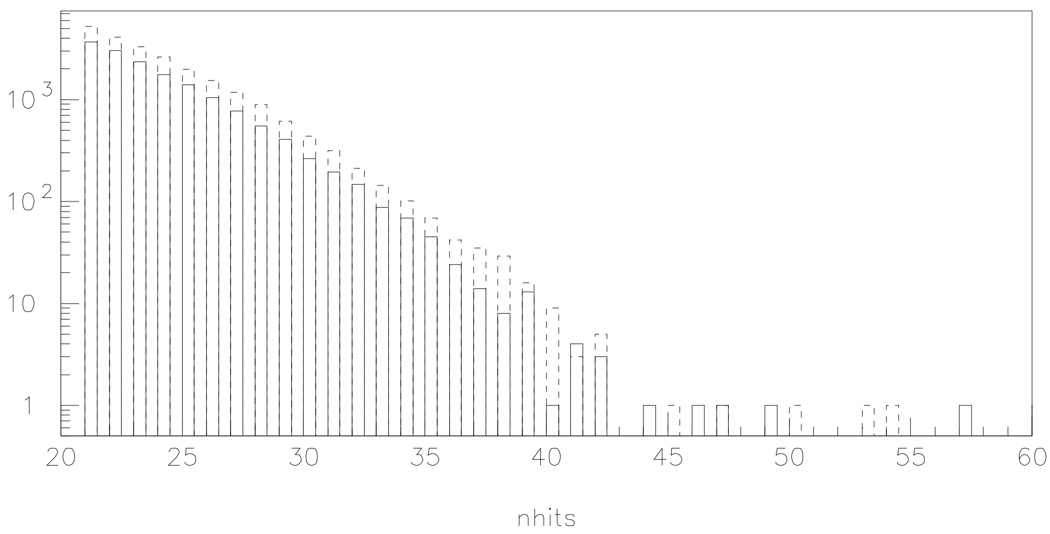

Figure 6: NHIT distributions for ^{208}Tl (upper plot) and ^{214}Bi (lower plot) decays with (dashed line) and without (solid line) a large acrylic source (radius 4cm, height 8cm).

indeed, if one looked in the range 25-35 hits the decays of ^{208}Tl are noticeably more isotropic than those of ^{214}Bi. He used an isotropy parameter, called "mean theta ij", defined by taking the mean of the angle between every pair of PMT hits with a fitted vertex taken as origin. This parameter is somewhat different to the one used in the CC/NC work, but encodes the same information, the differences between the two are merely the result of history and personal preference.

Crucial to the success of Chen's technique will be data sets of ^{208}Tl and ^{214}Bi decays in heavy water that will be used to produce isotropy PDFs, one for ^{208}Tl

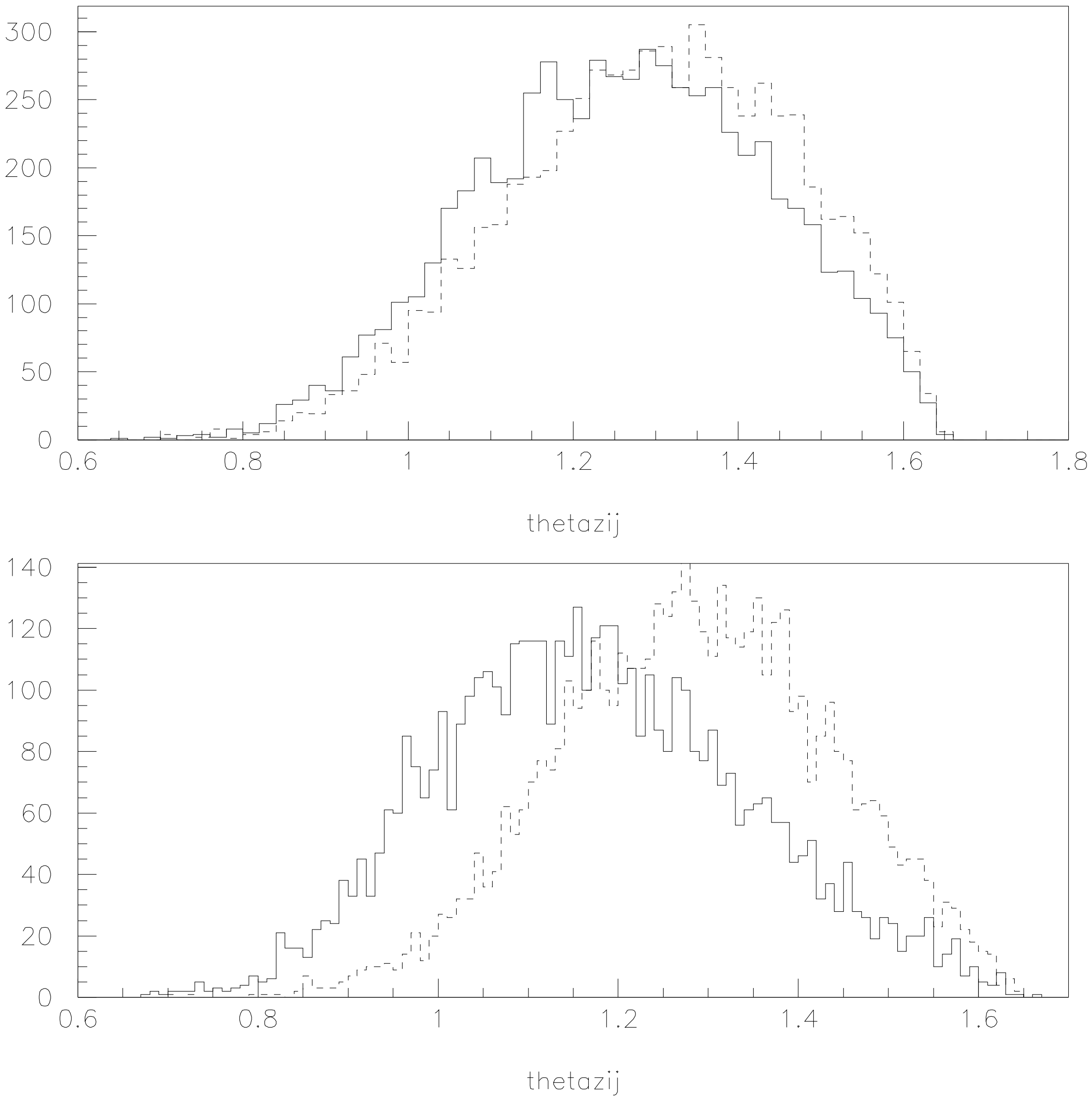

Figure 7: Theta_ij distributions for ^{208}Tl (upper plot) and ^{214}Bi (lower plot) decays with (dashed line) and without (solid line) the acrylic source.

and one for ^{214}Bi. The real data set isotropy histogram is then fit to a linear combination of these two PDFs and the contributions of ^{208}Tl and ^{214}Bi extracted. Ideally these PDFs would be formed directly from real calibration data and not directly use Monte Carlo at all. (This glosses over the question of how we know that such calibration data really does look like free ^{208}Tl and ^{214}Bi decays). If we are not able to produce such calibration sources we must resort to producing sources that look as much like free ^{208}Tl and ^{214}Bi decays as possible, ensuring that these sources are well mimicked by SNOMAN and then trusting SNOMAN to produce the PDF data sets. One powerful version of this scheme has the containerless U and Th sources that the water group is putting together verifying

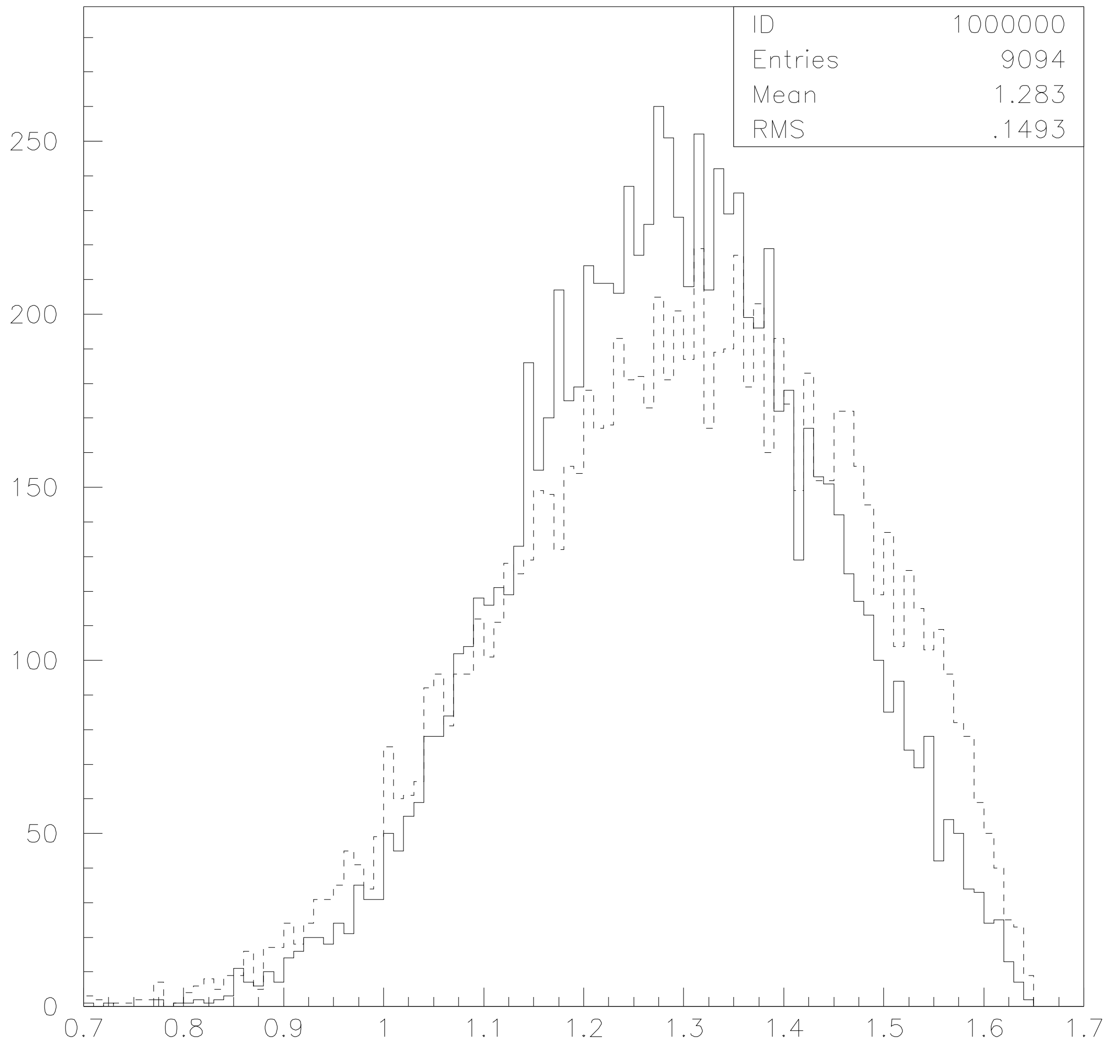

Figure 8: Theta_ij distributions for ^{208}Tl (dashed line) and ^{214}Bi (solid line) decays with the acrylic source. NHIT between 25 and 35

that we understand free ^{208}Tl and ^{214}Bi decays at the center of the vessel, with the encapsulated sources being used to show that we understand how these decays change appearance with changing radius.

Using an NHIT window of 25 - 35 hits and only those events that fit within 200cm of the source, Fig.7 shows the theta_ij distributions of ^{208}Tl and ^{214}Bi decays in water and in the acrylic source. It is clear that the presence of the source has a dramatic effect on the isotropy. Both isotopes are affected, but the ^{208}Tl less so as one would expect from the fact that much of its light originates in γs most of which will leave the acrylic before producing electrons.

Fig.8 shows that the clear separation between ^{208}Tl and ^{214}Bi events in water is all but obliterated by the presence of acrylic. A large part of the effect results from the NHIT shift induced by the acrylic. This shift means that a 25 to 35

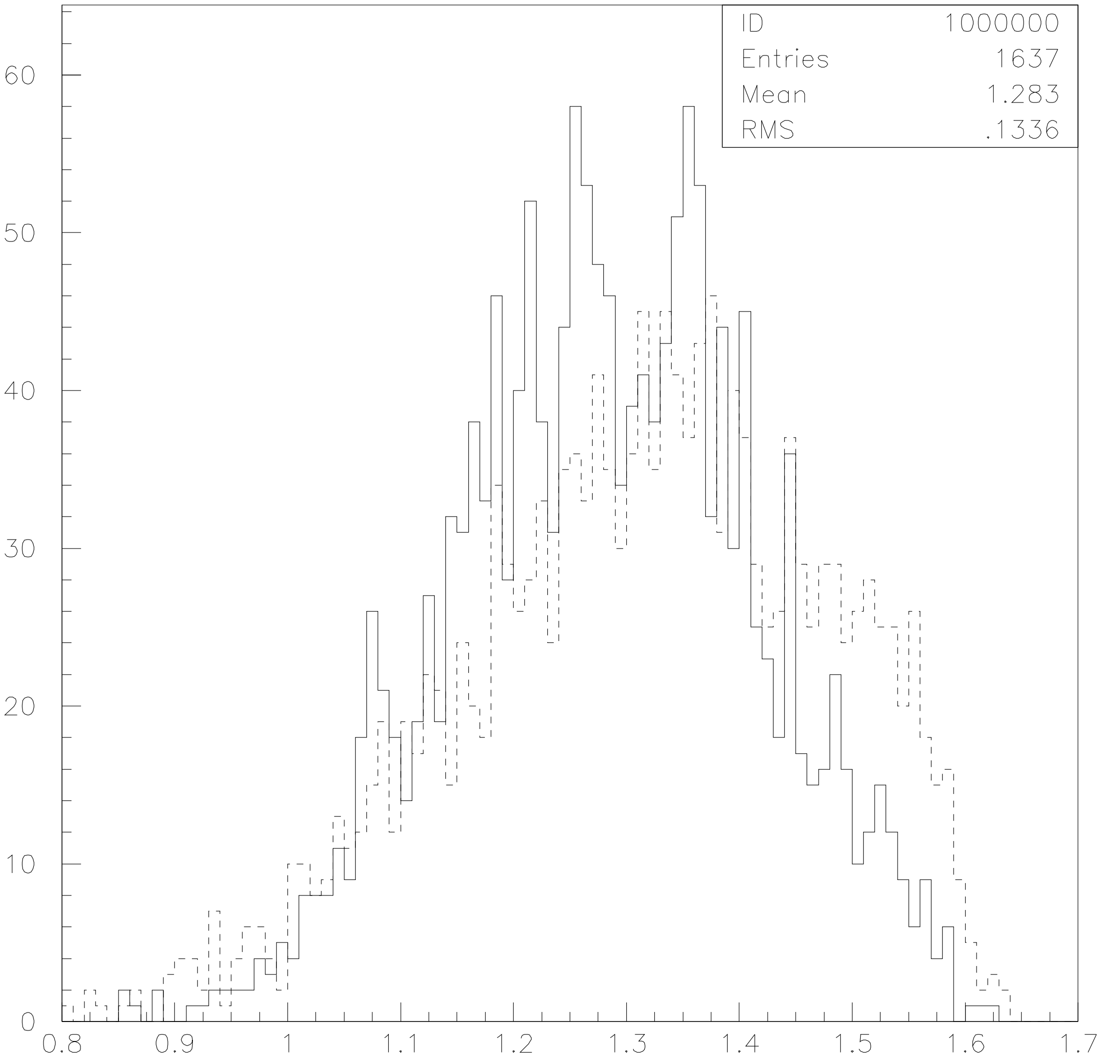

Figure 9: Theta_ij distributions for ^{208}Tl (dashed line) and ^{214}Bi (solid line) decays with the acrylic source. NHIT between 30 and 40

hit window now samples more of the low energy region where ^{208}Tl and ^{214}Bi look more like each other and are both more isotropic. To illustrate this effect Fig.9 shows the ^{208}Tl and ^{214}Bi theta_ij plots for the higher NHIT window of 30 - 40. Here ^{208}Tl and ^{214}Bi look more different, but not yet back to the differences shown by pure water decays. It is not clear what causes the remaining effect. It is likely to be either light scattering by the acrylic (as opposed to light extinction) or refraction at the acrylic/water interface. Further work needs to be done to study this.

Figs.7,8, and 9 show that, in their existing form, the acrylic encapsulated sources do not produce data that can be used to directly form isotropy PDFs. At best they can be used to calibrate SNOMAN and to point the way to future

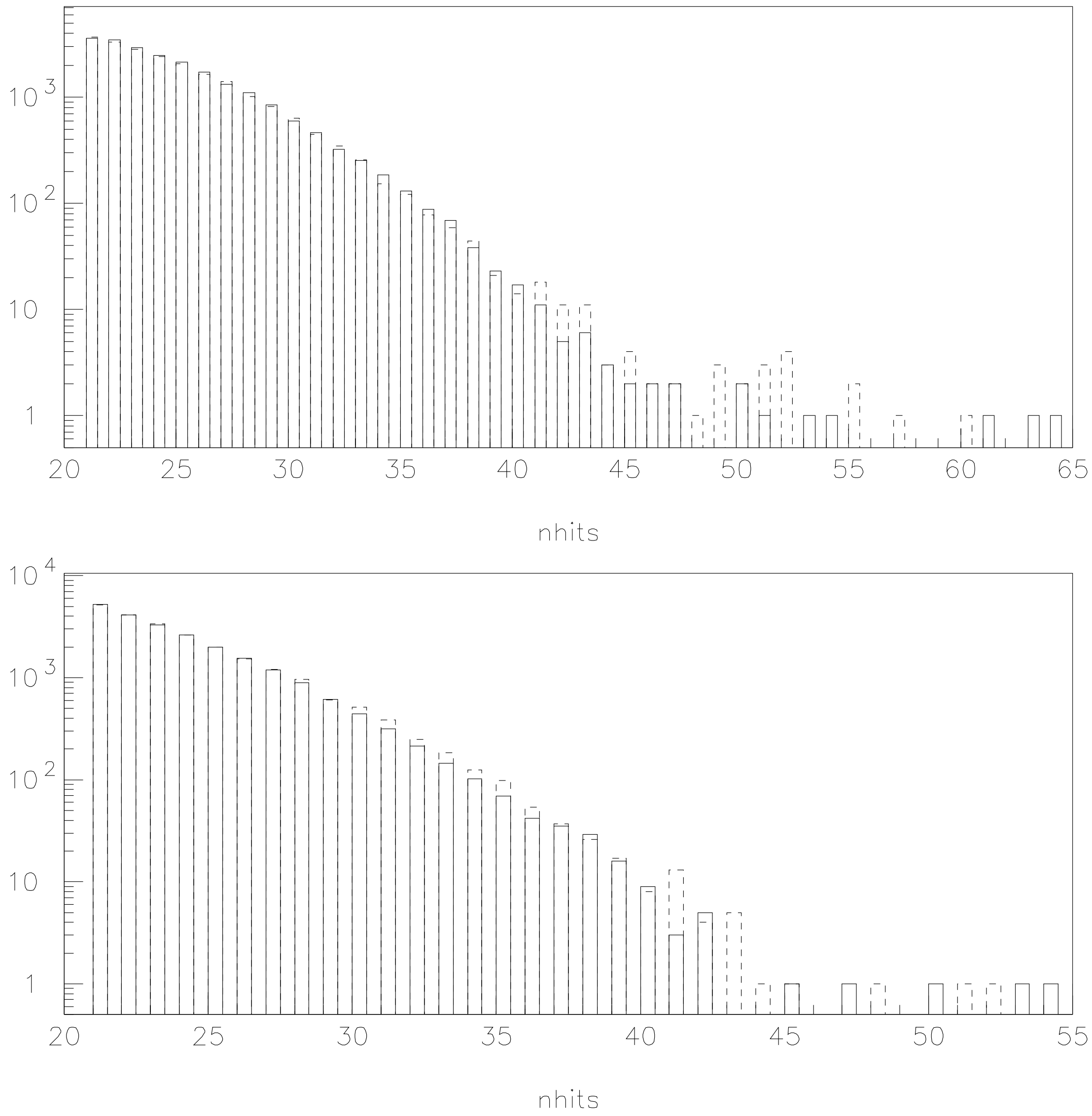

Figure 10: NHIT distributions for ^{208}Tl (upper plot) and ^{214}Bi (lower plot) decays produced by a cylindrical source (solid line) and a spherical source (dashed line)

redesigns.

3.3 The Effect of Source Shape

In order to see the effect of the shape of the acrylic on the NHIT and theta_ij spectra, simulations were also done with a spherical acrylic source of roughly the same volume as the cylindrical geometry. Figs.10 and 11 show that the differences between the two source geometries are minimal. One should not be too surprised by this. The electrons can travel up to about 1cm and so the Cerenkov light is

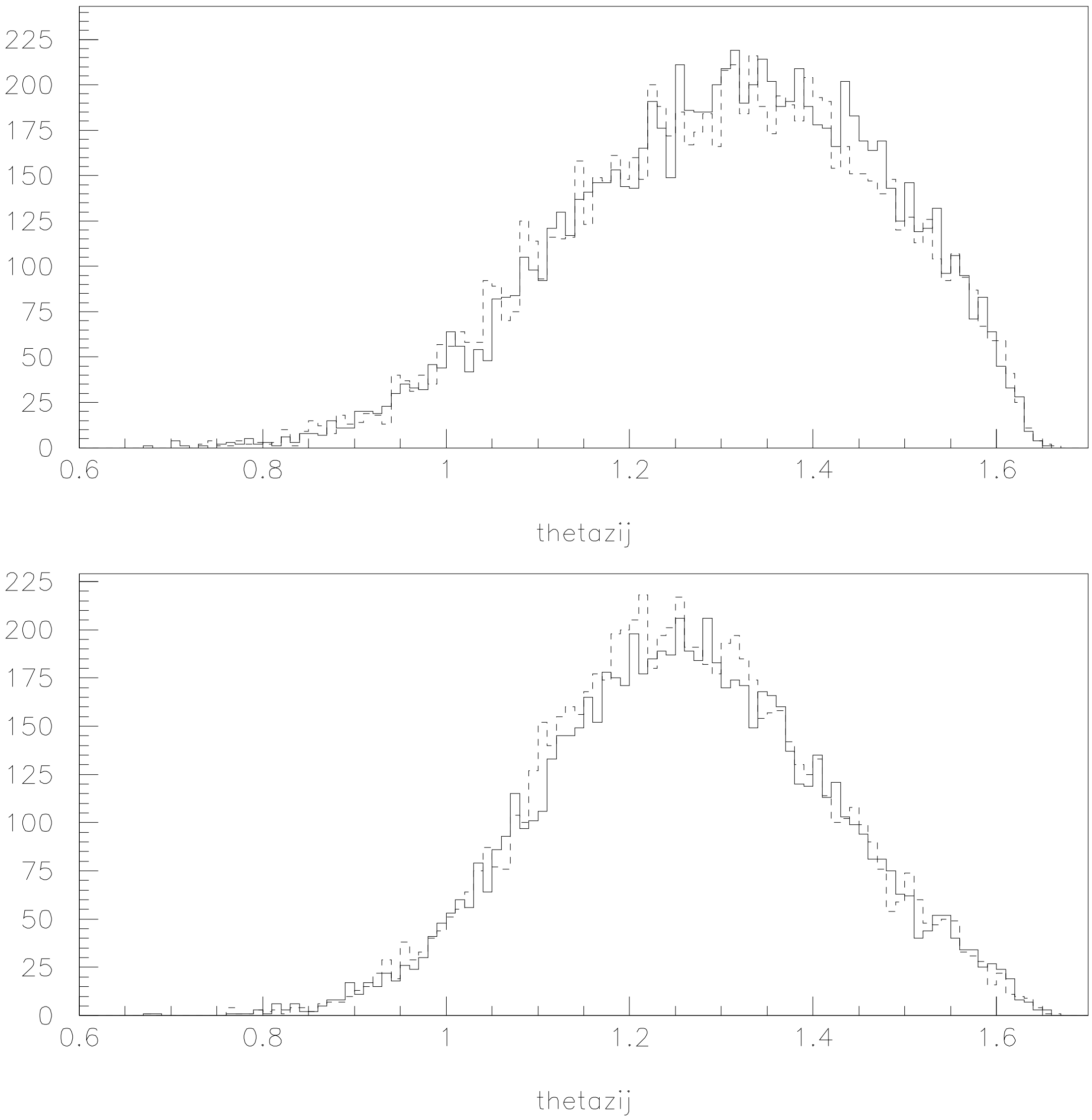

Figure 11: Theta_ij distributions for ^{208}Tl (upper plot) and ^{214}Bi (lower plot) decays produced by a cylindrical source (solid line) and a spherical source (dashed line)

not produced from the center, but rather from a central region that occupies a sizeable fraction of the source volume. This will tend to wash out any differences between the Cerenkov photon angles of incidence on the spherical and cylindrical boundaries, and consequently make any refractive effects look the same for the two geometries.

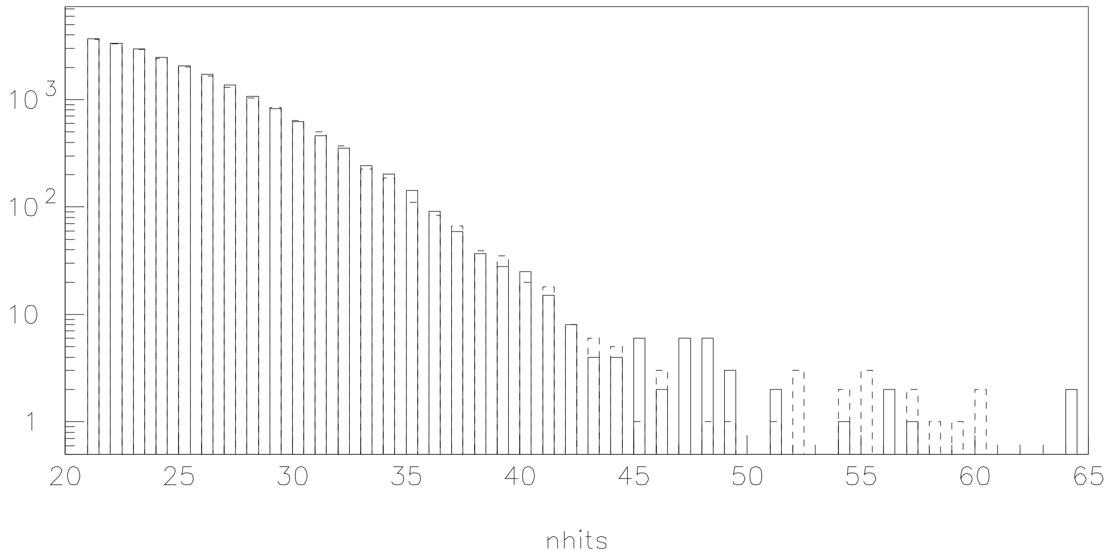

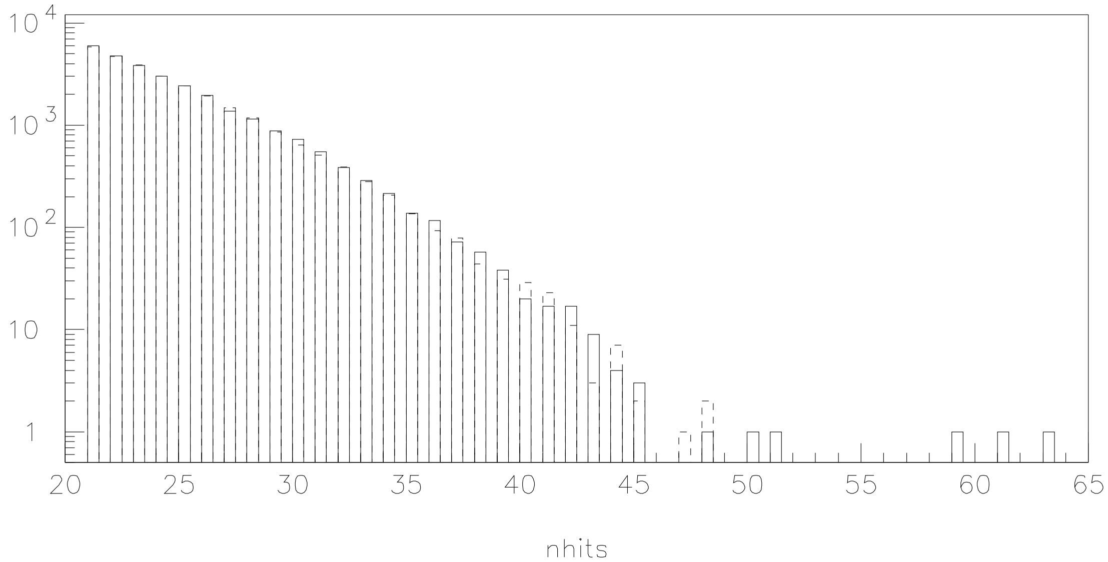

Figure 12: NHIT distributions for ^{208}Tl (upper plot) and ^{214}Bi (lower plot) decays produced by the source (solid line) and the source plus manipulator weight (dashed line)

3.4 The Effect of the Manipulator Weight

Figs.12 and 13 show the change in the NHIT and theta_ij spectra produced by introducing the manipulator weight into the simulation. The weight is modeled as 3.2cm radius, 26.4cm height lead cylinder encased in a thin layer of stainless and located with a 10cm gap above the source. This is not the correct mounting geometry being more obtrusive than the real thing. Given that the solid angle of the weight as viewed from the center of the source is only 2.4% it is no surprise that no noticeable effects show up in either NHITs or theta_ij.

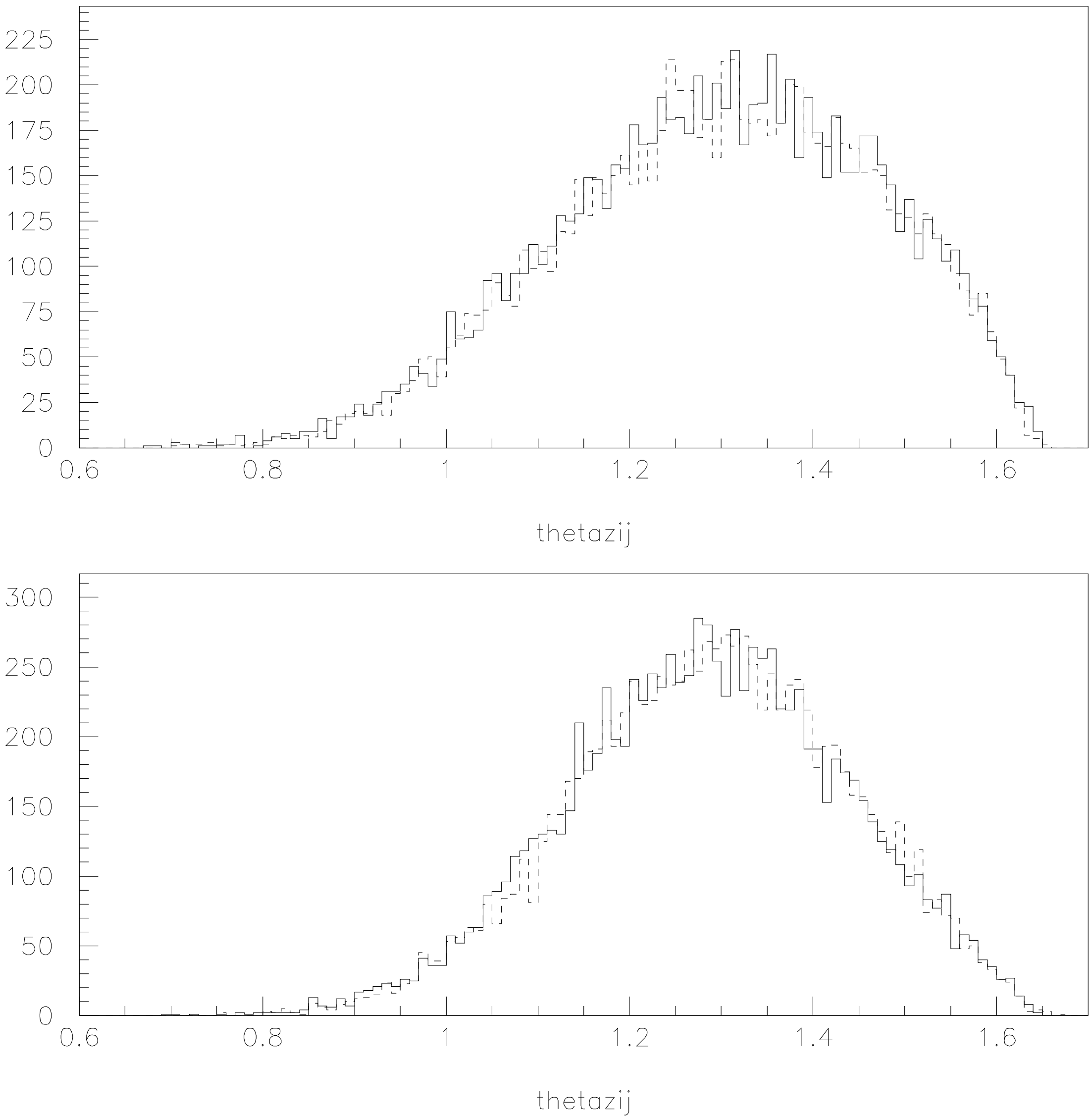

Figure 13: Theta_ij distributions for ^{208}Tl (upper plot) and ^{214}Bi (lower plot) decays produced by the source (solid line) and the source plus manipulator weight (dashed line)

3.5 The Effect of Bubbles

The existing acrylic encapsulated sources contain small bubbles, most likely shrink voids from the polymerisation process during fabrication. In an attempt, albeit an inaccurate one, to simulate the effects of such bubbles Figs. 14, 15, 16 and, 17 show the results on the NHIT and theta_ij spectra of incorporating

- A single 1cm radius spherical bubble at the center of the acrylic
- Two 0.5 cm spherical bubbles 0.6cm above and 0.6cm below the center

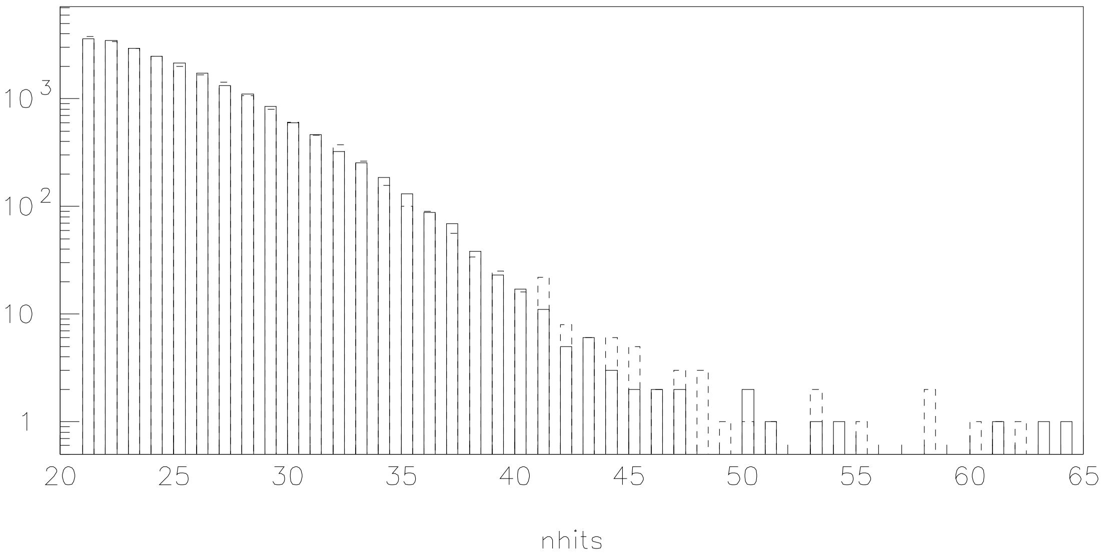

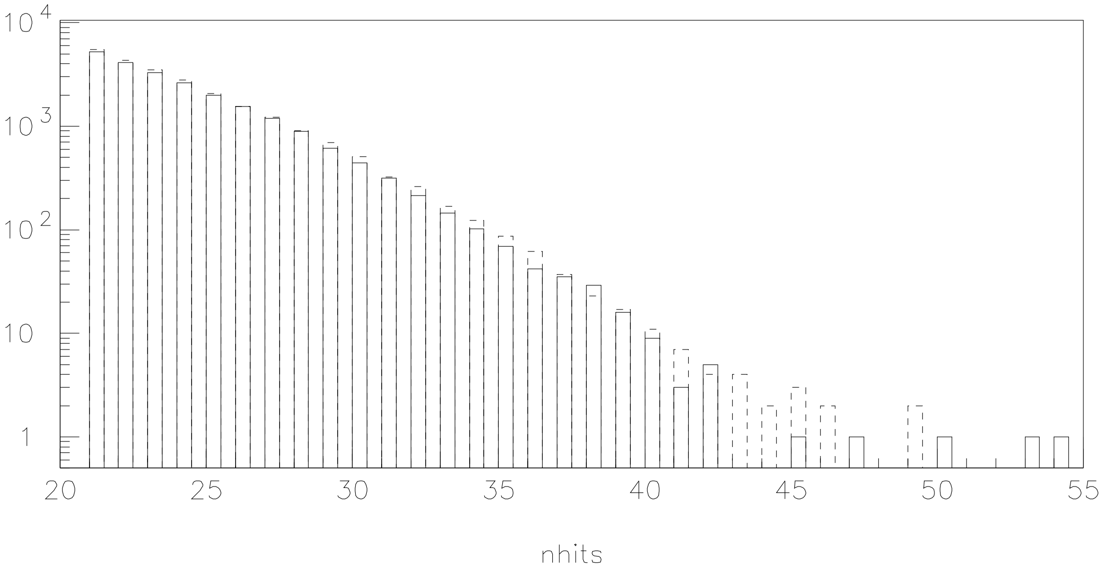

Figure 14: NHIT distributions for ^{208}Tl (upper plot) and ^{214}Bi (lower plot) decays produced by the source (solid line) and the source with a 1cm radius bubble at the center (dashed line)

For unfortunate historical reasons the source simulated here is larger than the real size, having a radius of 4cm and a height of 8cm. The fact that the single bubble shows no noticeable effects is no surprise as the Cerenkov light is only produced once the electron has exited the bubble and then tends to head outward and never encounter the air/acrylic interface. The two bubble simulation is a little more puzzling as one would expect to encounter refractive lensing effects, but none are seen. It is not understood why one's naive intuition is wrong in this case. Further simulations of more accurate bubbles can be done, but will we ever

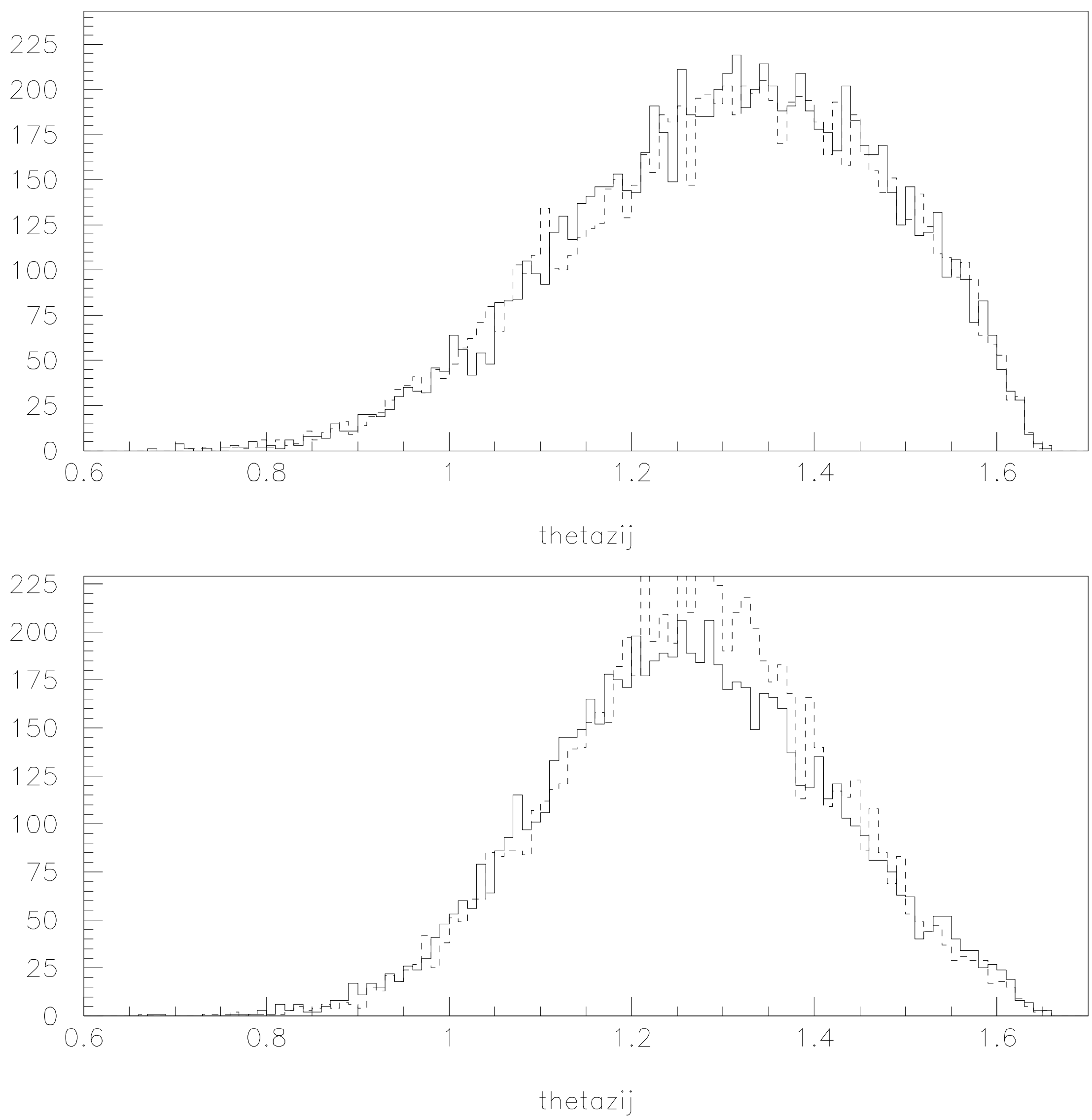

Figure 15: Theta_ij distributions for ^{208}Tl (upper plot) and ^{214}Bi (lower plot) decays produced by the source (solid line) and the source with a 1cm radius bubble at the center (dashed line)

be confident that the bubbles have no effect? It should not be too difficult to eliminate this source of possible error in the next generation of sources.

3.6 SNO Trigger Rate

Using the ^{16}N source it has been found that the builder cannot handle more than about 200Hz in trigger rate. For the low energy sources described here this rate should be higher since the NHIT spectrum is much lower, but 200hz still seems

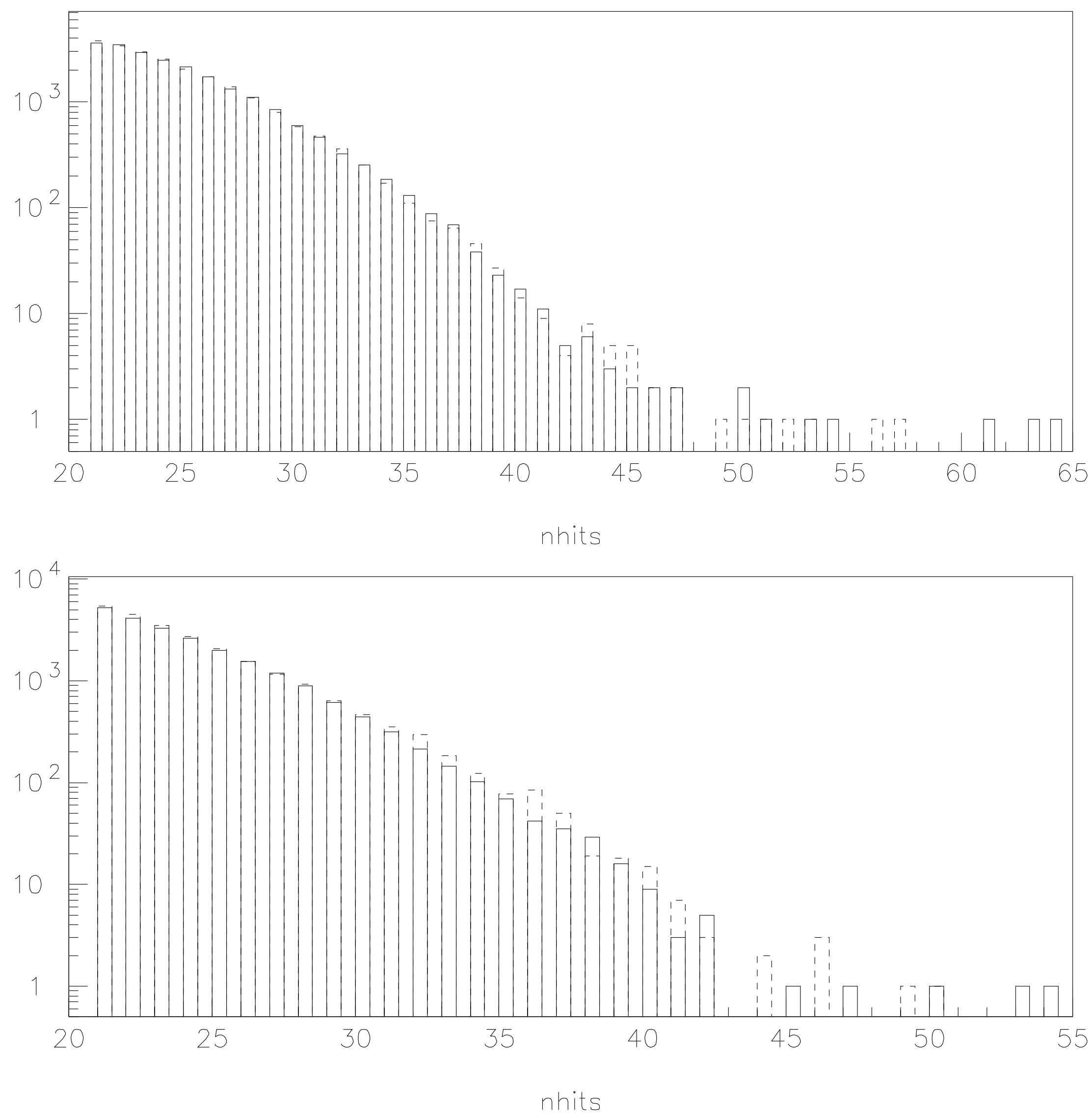

Figure 16: NHIT distributions for ^{208}Tl (upper plot) and ^{214}Bi (lower plot) decays produced by the source (solid line) and the source with two 0.5cm radius bubbles 0.6cm above and below the center (dashed line)

a safe limit to adopt. Since these are not-triggered sources, the higher their rate the higher the signal to background. This impels the sources to be run at as high a rate as possible.

Using SNOMAN 3_0186 this section makes predictions for the SNO trigger rate of the sources as a function of NHIT 100 MED threshold. Since it is know at the time of writing that SNOMAN's constants require adjustment to match real data, the results of this section should only be taken as guidelines. That being said, SNOMAN is at most 5% off in predicting the energy scale of ^{16}N and so the

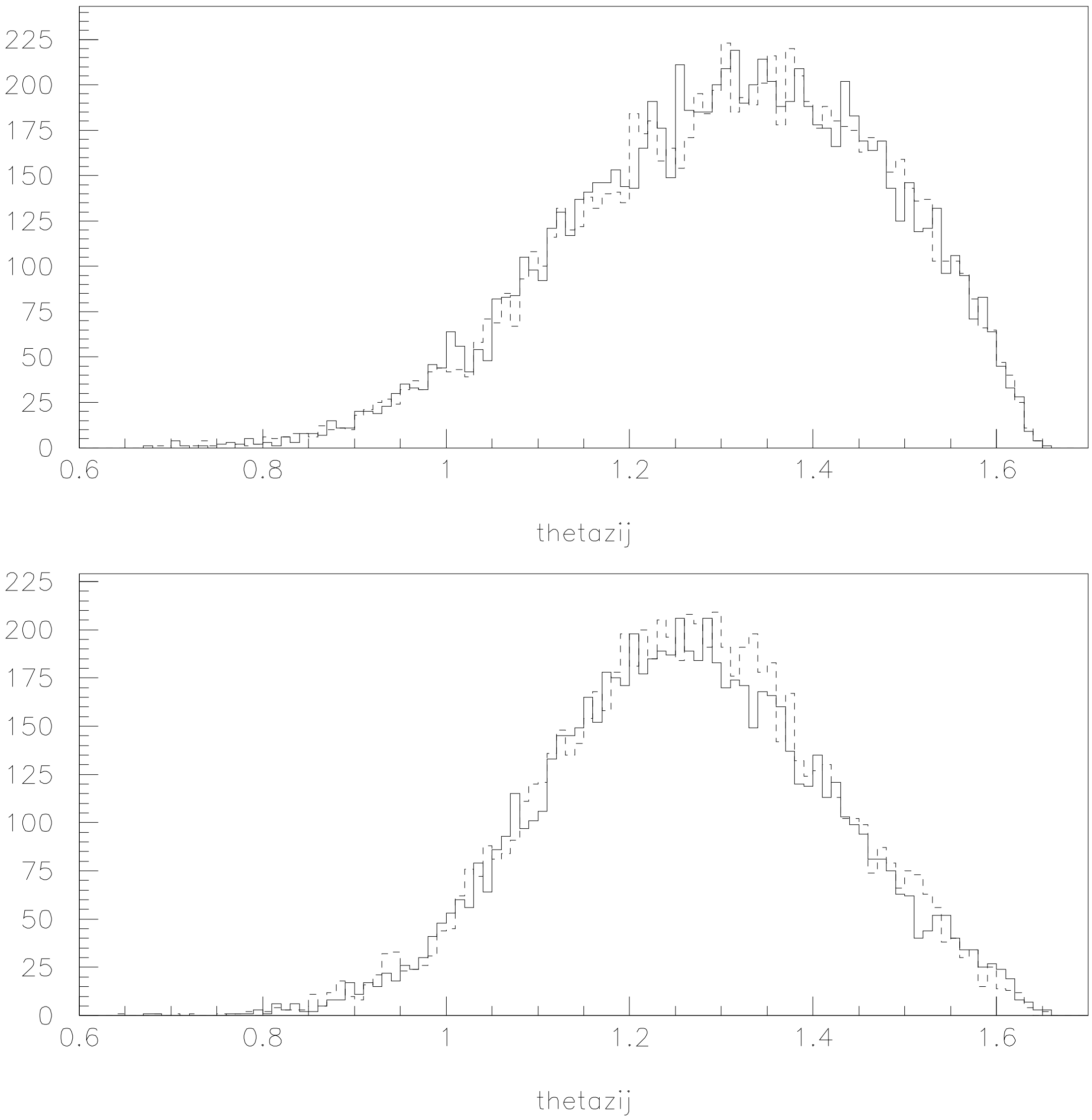

Figure 17: Theta_ij distributions for ^{208}Tl (upper plot) and ^{214}Bi (lower plot) decays produced by the source (solid line) and the source with two 0.5cm radius bubbles 0.6cm above and below the center (dashed line)

predictions here should not be too far off.

Below ^{228}Th in the Th chain (the level fed by the ^{232}U source) only ^{212}Bi and ^{208}Tl are at all likely to produce events of more than 10 hits. Shown in Fig.18 is the NHIT spectrum for 10000 cascades down the chain and the contributions of the 64% branching ratio ^{212}Bi and the 36% branching ratio ^{208}Tl. The table within this figure shows the probability for the two isotopes separately to get above a range of NHIT thresholds and the combined probability per cascade for this to happen (factoring in the isotope branching ratios).

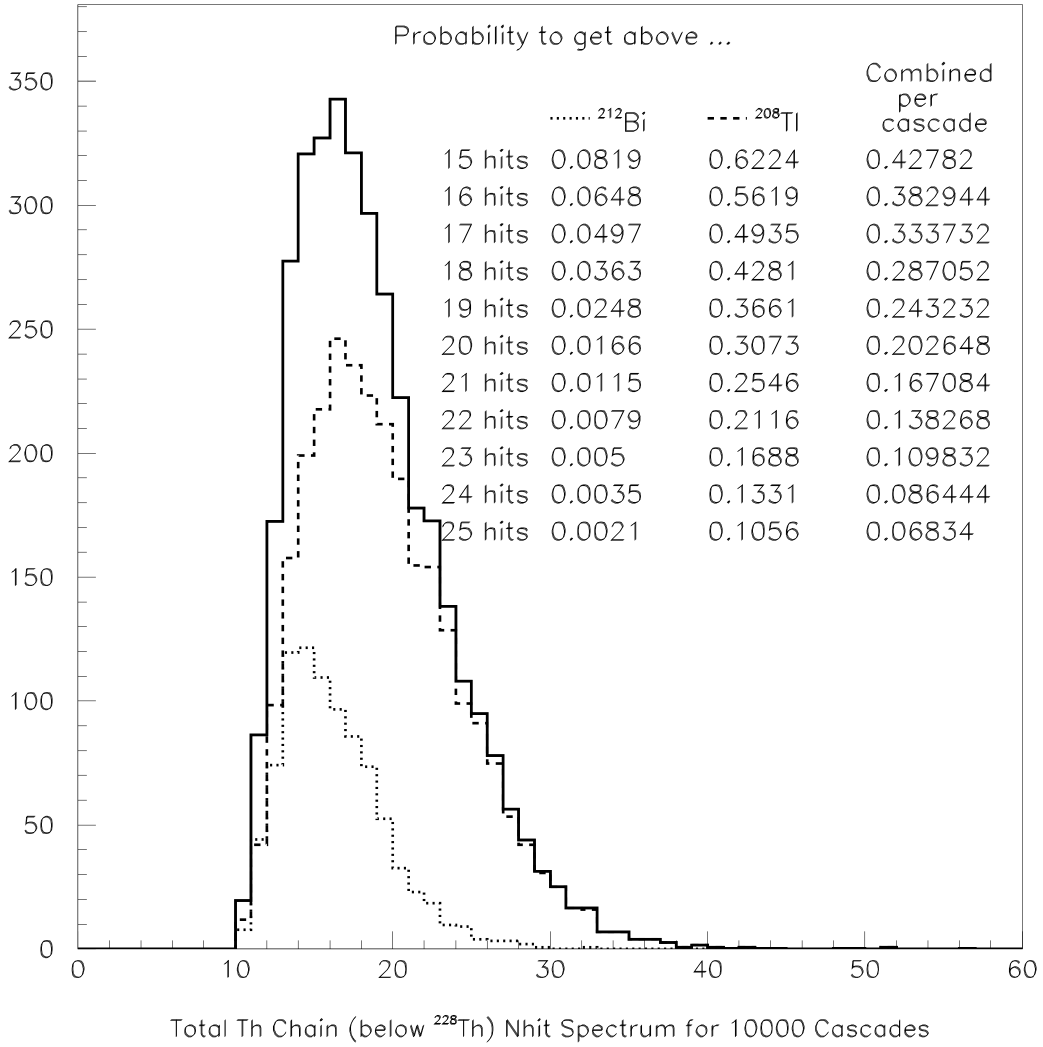

Figure 18: Source Th chain NHIT spectra and their efficiencies for triggering the detector

Below the ^{226}Ra source in the U chain only ^{214}Bi has any chance of getting above 10 hits (^{m234}Pa needs to be worried about in a real analysis, but is above ^{226}Ra in the chain). Fig.19 shows the NHIT spectrum from 10000 decays of ^{214}Bi. It's branching ratio is >99% and so this spectrum and the probability table beside it are also the cascade spectrum and probabilities per cascade.

The hot ^{232}U source has 5350 2.6MeV γs per second which implies $5350/0.36 = 14861$ cascades per second. Similarly the weak ^{232}U source has $99/0.36 = 275$ cascades per second. The branching ration for the 2.45 MeV γ in the ^{226}Ra source is 1.5% and so this source has $63/0.015 = 4200$ cascades per second. Multiplying

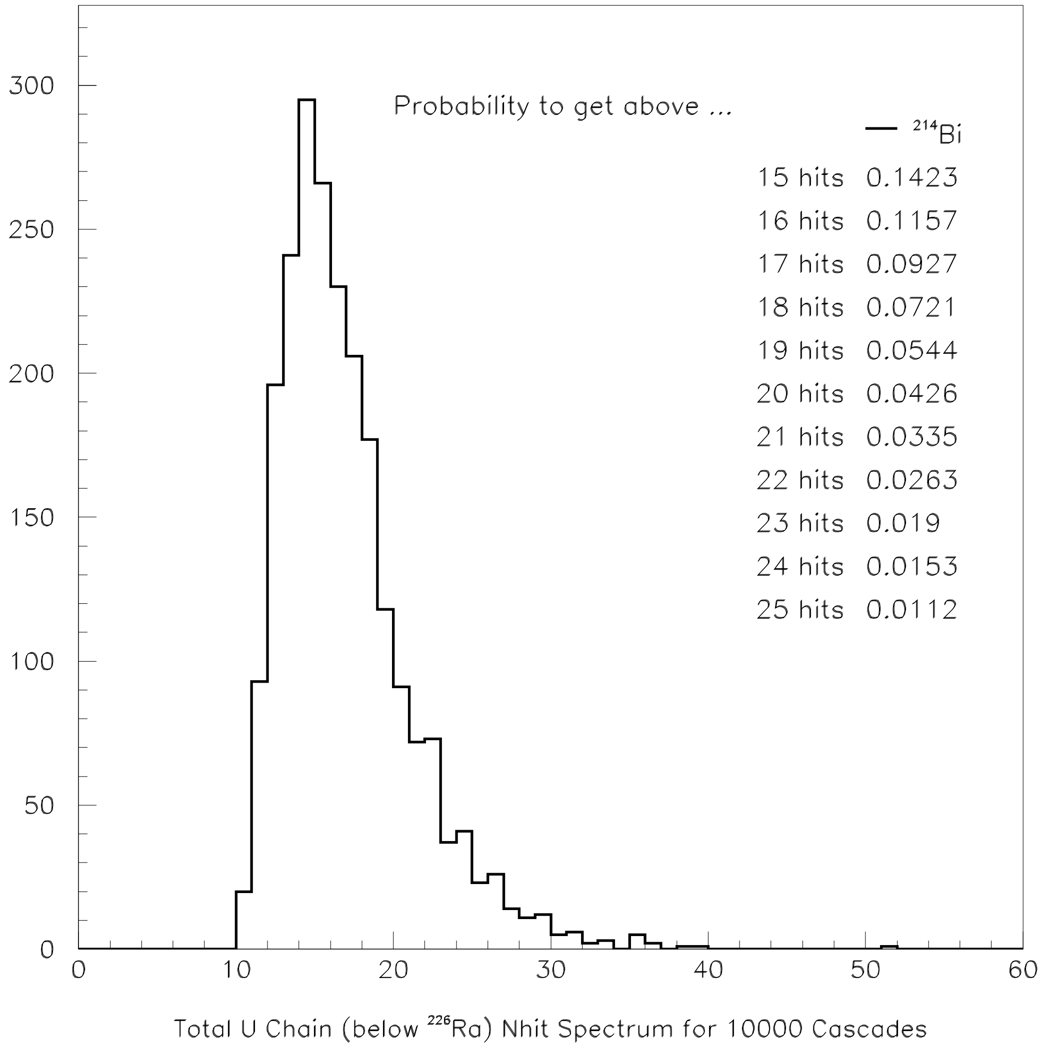

Figure 19: Source U chain NHIT spectra and their efficiencies for triggering the detector

these three numbers of cascades per second by their respective probabilities to breach a certain threshold enables Table 2 to be formed. This table gives the trigger rate for each source above a range of thresholds.

Several facts are clear from Table 2. The activity of the ^{226}Ra source is just about right to be used with an NHIT 100 trigger. At the time of writing the NHIT 100 MED trigger in SNO is set at 17 hits and has a rate of about 10Hz. Table 2 predicts that this would produce a raw signal to background ratio of 40:1 before any further cuts (e.g. fiducial volume). A higher ratio would be preferable and this should be born in mind when designing the next generation of sources. The higher rate could be handled by using either a prescaled trigger or by tuning the

NHIT Threshold	SNO Trigger Rate (Hz) ^{226}Ra	Hot ^{232}U	Weak ^{232}U
15 hits	598	6358	118
16 hits	486	5690	105
17 hits	389	4959	92
18 hits	303	4267	79
19 hits	228	3614	67
20 hits	179	3010	56
21 hits	141	2481	46
22 hits	110	2055	38
23 hits	80	1632	30
24 hits	64	1284	24
25 hits	47	1015	19

Table 2: SNO trigger rates and a function of threshold for each source

NHIT 20 trigger to effectively define a fiducial volume. The Hot ^{232}U source is far too strong to be used with an NHIT 100 trigger and probably even an NHIT 20 trigger. It will require the use of a prescaled trigger. Assuming a 17 hit threshold and a prescale of 25 this would produce a raw signal to background of about 500:1 - a very satisfactory figure. The Weak ^{232}U source is really too weak, with a raw signal to background predicted to be about 10:1. It may still be useful, however, as a general test of source principle if, for some reason, a prescaled trigger cannot be used with the Hot ^{232}U source. The source activities will clearly need some adjustment in the next generation of sources. The best approach will probably be to crank the source activity up and use a prescaled trigger, but it remains to be seen how the existing sources behave with a prescaled trigger and whether the risk of reduced supernova data is worth taking.

If one assumes, as a very rough guide, that the source rate in X. Chen's U/Th analysis window is about 50Hz then 1,000,000 events can be accumulated in this window in about 5.5 hours (i.e. about one shift).

4 Future Redesigns

It is clear from the preceding sections that a second generation of sources is needed if we are to meet the goals outlined in the Introduction. These new sources are constrained by two, usually conflicting, requirements:

1. The decays from these sources should look as much like free decays in water as possible.

2. There should be no possibility (within reason) of activity getting out of the

sources and into the heavy water.

Currently (before the first generation sources have gone in the detector) four lines of research are being pursued. These are described in the sections below.

4.1 Design 1: Smaller Sources

The differences between ^{208}Tl and ^{214}Bi decays in water and in the sources result from the acrylic material. The most obvious way the improve the next generation of sources would then be to reduce the amount of acrylic, so that the electrons leave the source quickly and generate most of their Cerenkov light in the water. One could consider just reducing the size of the first generation source design, but to reach the level of agreement between free and source decays one would need sources on the scale of a couple of millimeters. Whilst it may be possible to make sources on this scale, and it may even be possible to mount them securely, it is unlikely that we could come up with a design that we would consider safe from a radioactive contamination standpoint.

4.2 Design 2: Larger Sources

It was shown earlier in this report that the refractive index of acrylic boosts Cerenkov light production over that of water, but that the acrylic attenuation lowers it. These facts immediately lead to the possibility of adjusting the size of the acrylic sources so that the two effects cancel. This is worth pursuing because of its simplicity, but probably will not be sufficient for us since the spectrum of Cerenkov light coming out of the source will be different from that produced in water even if the normalizations can be matched.

4.3 Design 3: Heavy Water Bulb

The most obvious way to get ^{208}Tl and ^{214}Bi decays to look as if they are occurring in water is to let them occur in water. This could be achieved by placing the activity on a thin wire, stretching this wire across the inside of a hollow acrylic bulb, and filling the bulb with heavy water. Construction details like ensuring no air is trapped in the bulb could probably be overcome, and the bulb could be given a large enough radius to ensure that the electrons stayed within the water and that refractive effects at the water/acrylic boundaries were minimised. The question hanging over such a design is one of contamination safety. How does one either make the bulb reasonably unbreakable or ensure that no activity is released if the outer acrylic does break?

4.4 Design 4: Teflon AF

An alternative approach to the redesign question is to try to find a workable solid material with optical properties as close as possible to those of ultrapure water. Polymers typically have refractive indices between 1.4 and 1.5 compared to water's 1.33, but some searching has uncovered a candidate material - Teflon AF. Made by Dupont, it is described as being "highly transparent well into the UV". It has a refractive index of 1.31 at the sodium D line and this can be adjusted if it is not close enough. Being based on Teflon it is extremely chemically inert, but cannot be slush cast like acrylic. Instead it can be compression molded or deposited from flourinated solution. It is quite expensive, but the quantities needed are small and this should not present a problem. A sample has been obtained and optically tested by Chris Waltham and been shown to have transparencies comparable to those of UVT acrylic. One potential difficulty with this material is its relatively high density. This will stop electrons sooner than they would be stopped by water, and thus the Cerenkov photon production may be significantly below that of water. This is potentially a material of some importance to SNO. One could see it being used in a number of calibration sources, in particular the ^{8}Li source. Anyone interested should contact Steve Brice for more information.

5 Conclusion

This document has provided details on the first generation of acrylic encapsulated low energy sources. It is not complete and more work needs to be done, particularly in understanding the optical response of the existing sources. It is clear, however, that these existing sources will not provide all the information we need in sufficient detail. A next generation of sources is required and the last section has indicated some of the forms such a redesign might take.